

# **On the importance of low-dimensional structures for data-driven modeling**

Jean-Christophe Loiseau

May, 13<sup>th</sup> 2022

- Maître de Conférences in Fluid Dynamics and Applied Math.
- Machine-learning enthusiast with application to engineering systems.
- Data-efficient models with guarantees of optimality or interpretability.





## **A brief overview of SVD**

$$\mathbf{A} = \mathbf{U} \mathbf{\Sigma} \mathbf{V}^T$$

Basis for colspan( $A$ )

Basis for rowspan( $A$ )

$$A = U \Sigma V^T$$

Diagonal matrix

## Relation to spectral decomposition

$$\begin{bmatrix} \mathbf{0} & \mathbf{A} \\ \mathbf{A}^T & \mathbf{0} \end{bmatrix} \begin{bmatrix} \mathbf{u}_i \\ \mathbf{v}_i \end{bmatrix} = \sigma_i \begin{bmatrix} \mathbf{u}_i \\ \mathbf{v}_i \end{bmatrix}$$

Generalization of the *eigenvalue decomposition* to **non-square matrices** by E. Beltrami (1873) and C. Jordan (1874). The first efficient numerical algorithm was developed by G. Golub *et al.* in the late 1960s.

## Schematic of SVD

# Ordinary least-squares

$$y = ax + b$$



# Ordinary least-squares

$$\underset{a,b}{\text{minimize}} \sum_{i=1}^N (y_i - ax_i - b)^2$$


# Ordinary least-squares

$$\underset{x}{\text{minimize}} \quad \|Ax - b\|_2^2$$

# Ordinary least-squares

$$x = (A^T A)^{-1} A^T b$$

Moore-Penrose  
pseudoinverse



$$\mathbf{A}^\dagger = (\mathbf{A}^T \mathbf{A})^{-1} \mathbf{A}^T$$

$$\mathbf{A}^\dagger = (\mathbf{V}\Sigma\mathbf{U}^T\mathbf{U}\Sigma\mathbf{V}^T)^{-1} \mathbf{V}\Sigma\mathbf{U}^T$$

$$\mathbf{A}^\dagger = \mathbf{V}\mathbf{\Sigma}^{-1}\mathbf{U}^T$$

$$\sigma_i^{-1} = \begin{cases} \frac{1}{\sigma_i} & \text{if } \sigma_i > \varepsilon \\ 0 & \text{otherwise.} \end{cases}$$

- `np.linalg.lstsq(A, b)`
- `A\b`

# Low-rank approximation

How to compress this image ?



# Low-rank approximation

$$\begin{array}{ll} \underset{\mathbf{X}}{\text{minimize}} & \|\mathbf{A} - \mathbf{X}\|_F^2 \\ \text{subject to} & \text{rank } \mathbf{X} = r \end{array}$$

# Low-rank approximation

Singular value distribution

# Low-rank approximation

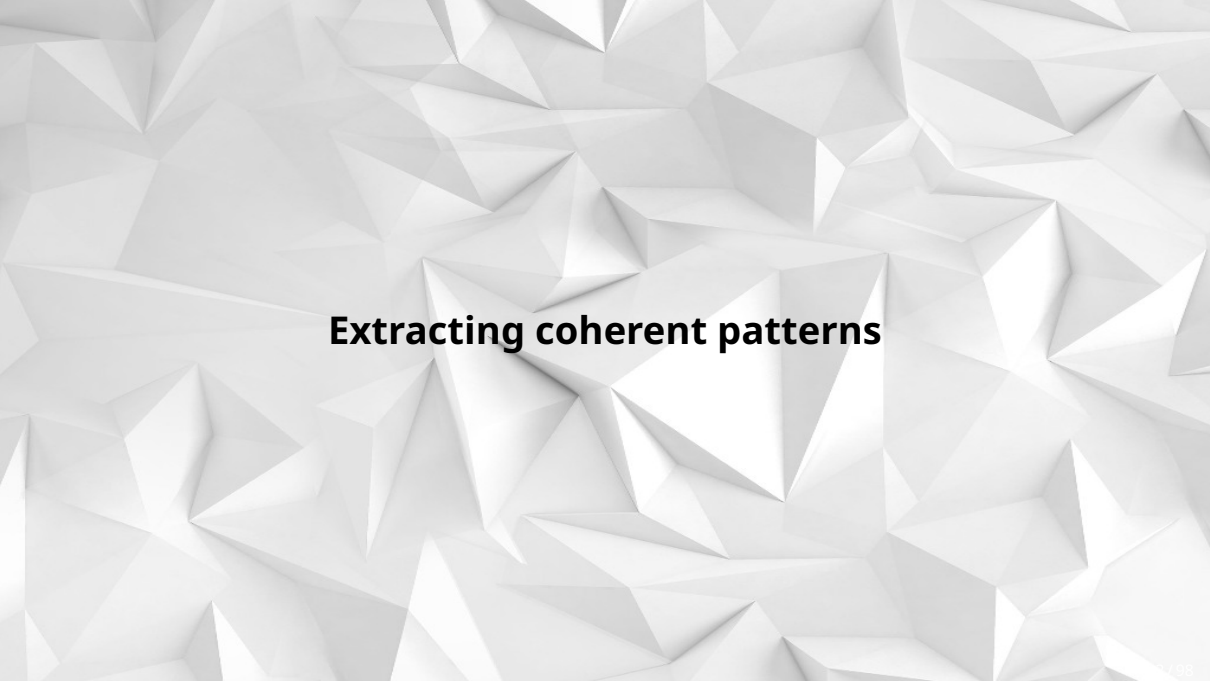
Reconstructed image for different rank

# Low-rank approximation

Canonical images

# Low-rank approximation

Image with more fine scale details



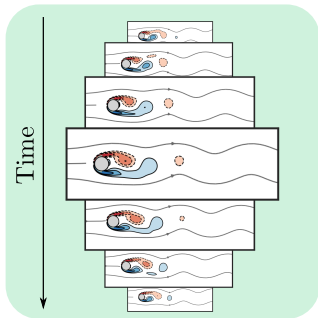
## **Extracting coherent patterns**

Add Yale B faces

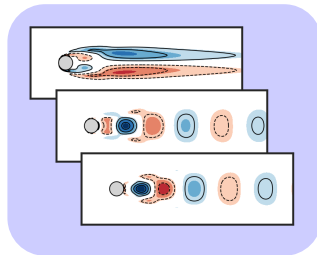
Add video of the cavity



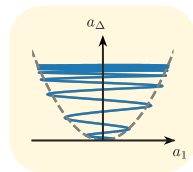
Navier-Stokes simulation

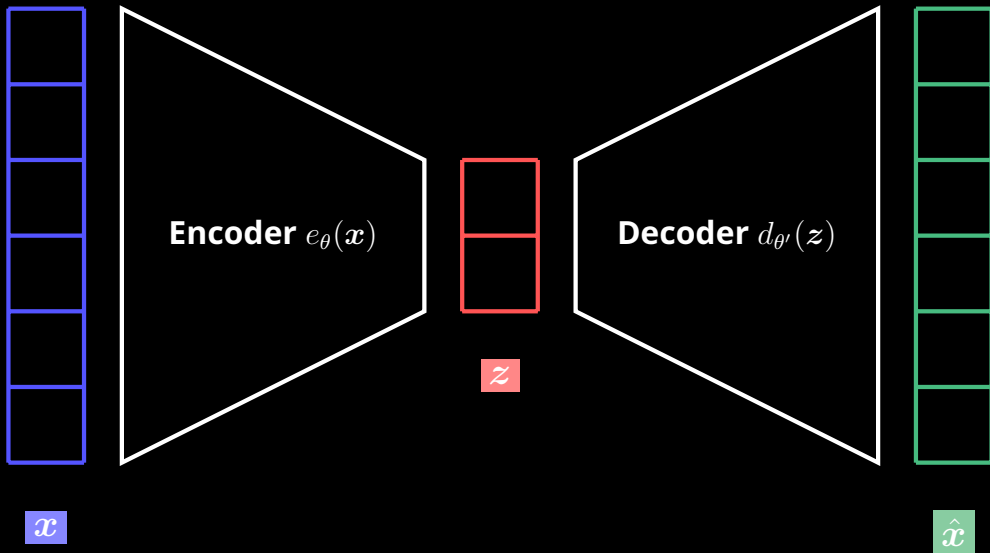


Dimensionality reduction



Simple representation





$$\min_{\theta, \theta'} \sum_{i=1}^N \left\| \underbrace{x_i}_{\text{Ground truth}} - \underbrace{(d_{\theta'} \circ e_{\theta})(x_i)}_{\text{Estimate}} \right\|_2^2$$

$$\begin{array}{ll}
\underset{\mathbf{P}, \mathbf{Q}}{\text{minimize}} & \sum_{i=1}^N \|\mathbf{x}_i - \mathbf{P}\mathbf{Q}^T \mathbf{x}_i\|_2^2 \\
\text{subject to} & \text{rank } \mathbf{P} = \text{rank } \mathbf{Q} = r
\end{array}$$

$$\begin{array}{ll} \underset{\boldsymbol{P}}{\text{minimize}} & \sum_{i=1}^N \|\boldsymbol{x}_i - \boldsymbol{P}\boldsymbol{P}^T \boldsymbol{x}_i\|_2^2 \\ \text{subject to} & \text{rank } \boldsymbol{P} = r \end{array}$$

$$\begin{array}{ll} \underset{\mathbf{P}}{\text{minimize}} & \|\mathbf{X} - \mathbf{P}\mathbf{P}^T\mathbf{X}\|_F^2 \\ \text{subject to} & \mathbf{P}^T\mathbf{P} = \mathbf{I}_r \end{array}$$

## Proper Orthogonal Decomposition

$$P\Lambda = C_{xx}P$$

$P$  corresponds to the left singular vectors of  $X$ . The latent representation is given by  $z_i = P^T x_i$ . The optimal rank of the model can be inferred from the distribution of the PCA eigenvalues  $\Lambda = \Sigma^2$ .

# Eigenfaces



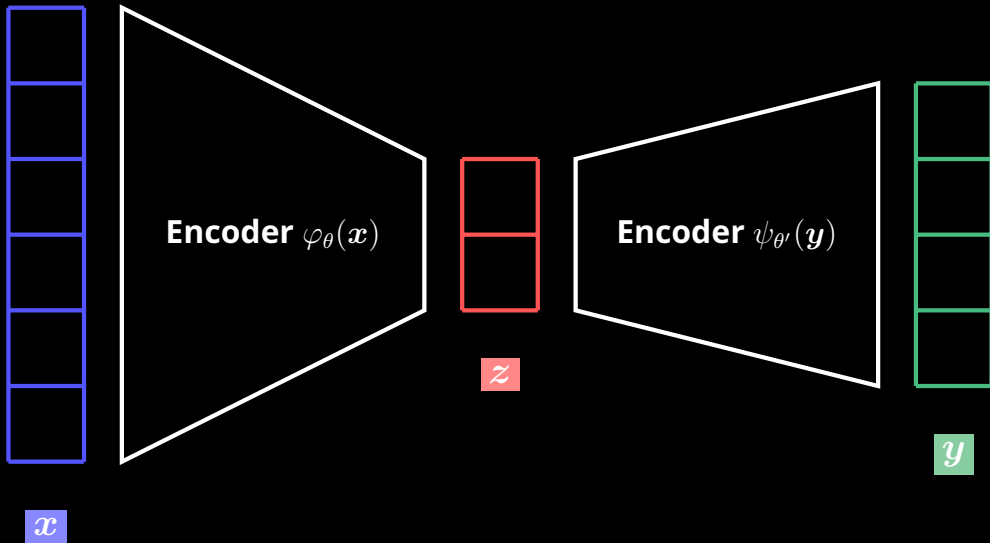
# Shear-driven cavity POD modes

Add POD modes

# Shear-driven cavity POD modes

Add phase portraits

Add cylinder flow and pressure coefficient



$$\min_{\theta, \theta'} \sum_{i=1}^N \|\varphi_{\theta}(\mathbf{x}_i) - \psi_{\theta'}(\mathbf{y}_i)\|_2^2$$

$$\begin{array}{ll}
\underset{\mathbf{P}, \mathbf{Q}}{\text{minimize}} & \sum_{i=1}^N \|\mathbf{P}^T \mathbf{y}_i - \mathbf{Q}^T \mathbf{x}_i\|_2^2 \\
\text{subject to} & \text{rank } \mathbf{P} = \text{rank } \mathbf{Q} = r
\end{array}$$

$$\begin{array}{ll}
\underset{P, Q}{\text{minimize}} & \|P^T Y - Q^T X\|_F^2 \\
\text{subject to} & P^T C_{yy} P = Q^T C_{xx} Q = I_r
\end{array}$$

## Canonical Correlation Analysis

$$\begin{bmatrix} C_{yy} & 0 \\ 0 & C_{xx} \end{bmatrix} \begin{bmatrix} P \\ Q \end{bmatrix} \Sigma = \begin{bmatrix} 0 & C_{yx} \\ C_{xy} & 0 \end{bmatrix} \begin{bmatrix} P \\ Q \end{bmatrix}$$

CCA relies on a *generalized eigenproblem*.  $P$  and  $Q$  describe the encoders such that the latent representations  $z = Q^T x$  and  $z' = P^T Y$  are as similar as possible. It is closely related to the concept of *mutual information*.



Add cylinder flow and pressure coefficient

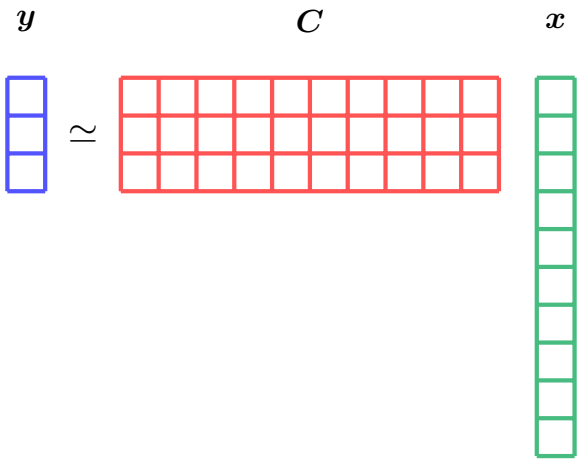
# **Optimal sensor placement**

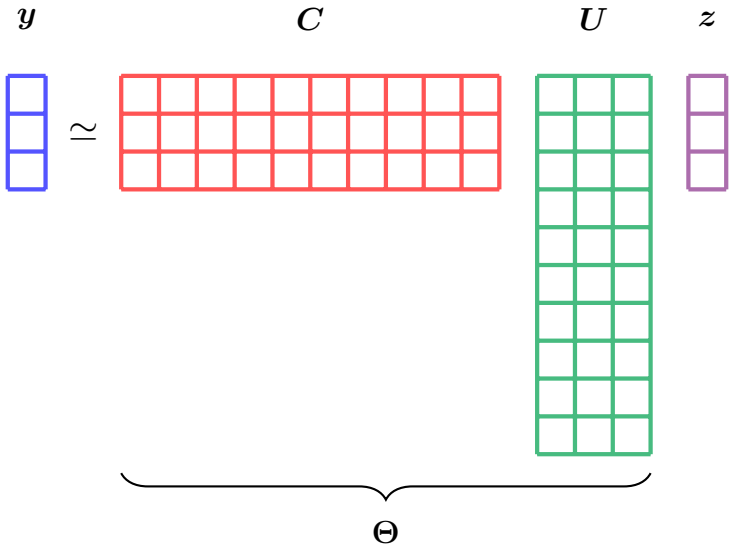


Measurement operator

$$\underset{\text{Observations}}{y} = \underset{\text{Full state}}{C} x$$

The diagram illustrates the measurement equation  $y = Cx$ . The variable  $y$  is enclosed in a blue square, with a blue arrow pointing from the underlined label "Observations" below to it. The variable  $x$  is enclosed in a green square, with a green arrow pointing from the underlined label "Full state" below to it. The matrix  $C$  is enclosed in a red square, with a red arrow pointing from the underlined label "Measurement operator" above to it. The equals sign is positioned between the blue and red squares.





$$\begin{array}{ccc}
 y & \mathbf{I} & z \\
 \begin{array}{|c|} \hline \\ \hline \\ \hline \\ \hline \end{array} & \approx & \begin{array}{|c|c|c|} \hline & & \\ \hline & & \\ \hline & & \\ \hline \end{array} \begin{array}{|c|} \hline \\ \hline \\ \hline \\ \hline \end{array}
 \end{array}$$

$$\underset{\mathbf{z}}{\text{minimize}} \quad \|\mathbf{y} - \Theta \mathbf{z}\|_2$$



$$z = \Theta^{-1}y$$

$$\underset{\boldsymbol{C}}{\text{maximize}} \quad |\det(\boldsymbol{C}\boldsymbol{U})|$$

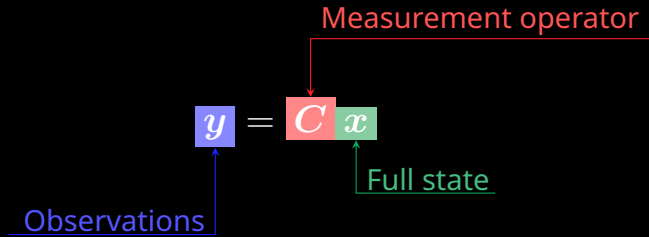
$$\begin{array}{ll}
\underset{\mathbf{C}}{\text{maximize}} & |\det(\mathbf{C}\mathbf{U})| \\
\text{subject to} & \mathbf{C}_i \in \{\mathbf{e}_j\}_{j=1,n}
\end{array}$$

QR sensor placement algorithm

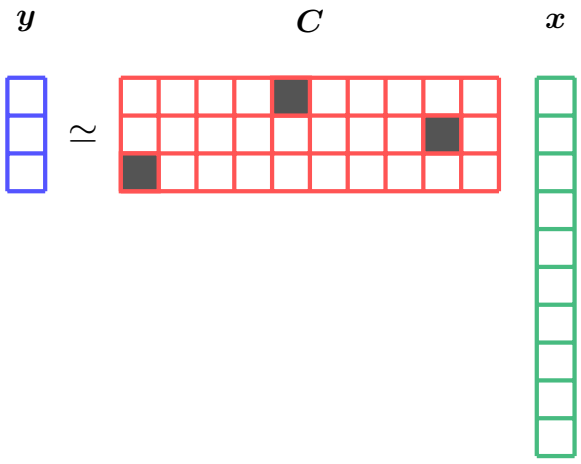
# Extended Yale B Face dataset

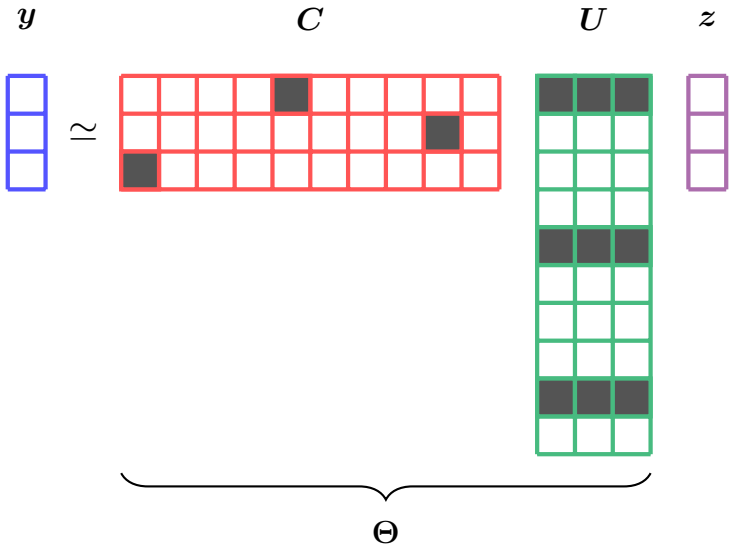
# Shear-driven cavity flow

# **State estimation and low-rank sensing**









$$\begin{array}{c}
 \mathbf{y} \qquad \qquad \mathbf{I} \qquad \qquad \mathbf{z} \\
 \begin{array}{|c|} \hline \\ \hline \\ \hline \\ \hline \end{array}
 \quad
 \begin{array}{c} \approx \\ \sim \end{array}
 \quad
 \begin{array}{|c|c|c|} \hline & & \\ \hline & & \\ \hline & & \\ \hline \end{array}
 \quad
 \begin{array}{|c|} \hline \\ \hline \\ \hline \\ \hline \end{array}
 \end{array}$$

### Undertermined problem

$$\begin{array}{ll} \underset{z}{\text{minimize}} & \|z\|_2 \\ \text{subject to} & \mathbf{y} = \Theta z \end{array}$$

### Overdetermined problem

$$\underset{z}{\text{minimize}} \quad \|\mathbf{y} - \Theta z\|_2^2$$

## Regularized problem

$$\underset{\mathbf{z}}{\text{minimize}} \quad \|\mathbf{y} - \Theta \mathbf{z}\|_2^2 + \lambda \|\mathbf{z}\|_2^2$$

## Regularized and constrained problem

$$\begin{array}{ll} \underset{\mathbf{z}}{\text{minimize}} & \|\mathbf{y} - \Theta \mathbf{z}\|_2^2 + \lambda \|\mathbf{z}\|_2^2 \\ \text{subject to} & |z_i| \leq 2\sigma_i \quad \forall i \end{array}$$

Add figures from SIAM paper



# **Reduced-order modeling**





Natural dynamics

Actuators

$$\frac{dx}{dt} = \boxed{A}x + \boxed{B}u$$

$$y = \boxed{C}x + \boxed{D}u$$

Measurements

Feedthrough

## Controllability Gramian

$$\mathbf{W}_c = \int_0^{\infty} e^{\tau \mathbf{A}} \mathbf{B} \mathbf{B}^* e^{\tau \mathbf{A}^*} d\tau$$

## Observability Gramian

$$\mathbf{W}_O = \int_0^{\infty} e^{\tau \mathbf{A}^*} \mathbf{C}^* \mathbf{C} e^{\tau \mathbf{A}} d\tau$$

### Cross Gramian

$$\mathbf{W}_x = \int_0^{\infty} e^{\tau A} \mathbf{B} \mathbf{C} e^{\tau A} d\tau$$

$$\begin{array}{ll} \underset{\boldsymbol{U}, \boldsymbol{V}}{\text{maximize}} & \text{Tr}(\boldsymbol{U}^* \boldsymbol{W}_{\mathcal{X}} \boldsymbol{V}) \\ \text{subject to} & \boldsymbol{U}^* \boldsymbol{U} = \boldsymbol{V}^* \boldsymbol{V} = \boldsymbol{I}_r \end{array}$$

## Sylvester equation<sup>1</sup>

$$AW_{\mathcal{X}} + W_{\mathcal{X}}A = -BC$$

---

<sup>1</sup>Its resolution is tractable only for low-dimensional systems.

## Balanced Proper Orthogonal Decomposition

1. For each actuator, compute the corresponding impulse response

$$\mathbf{X}_i = [\mathbf{B}_i \quad e^{\Delta t \mathbf{A}} \mathbf{B}_i \quad e^{2\Delta t \mathbf{A}} \mathbf{B}_i \quad \dots \quad e^{n\Delta t \mathbf{A}} \mathbf{B}_i]$$

and assemble the data matrix  $\mathbf{X} = [\mathbf{X}_1 \quad \mathbf{X}_2 \quad \dots \quad \mathbf{X}_p]$ .



## Balanced Proper Orthogonal Decomposition

2. For each sensor, compute the corresponding **adjoint** impulse response

$$\mathbf{Y}_i = [\mathbf{C}_i^* \quad e^{\Delta t \mathbf{A}^*} \mathbf{C}_i^* \quad e^{2\Delta t \mathbf{A}^*} \mathbf{C}_i^* \quad \dots \quad e^{n\Delta t \mathbf{A}^*} \mathbf{C}_i^*]$$

and assemble the data matrix  $\mathbf{Y} = [\mathbf{Y}_1 \quad \mathbf{Y}_2 \quad \dots \quad \mathbf{Y}_q]$ .

## Balanced Proper Orthogonal Decomposition

3. Approximate the cross Gramian  $W_{\mathcal{X}}$  as

$$W_{\mathcal{X}} \simeq XY^T.$$

where  $X$  and  $Y$  are the data matrices obtained in the previous steps.

## Petrov-Galerkin projection

$$\begin{aligned}\frac{d\hat{x}}{dt} &= \hat{A}\hat{x} + \hat{B}u \\ \hat{y} &= \hat{C}\hat{x} + \hat{D}u\end{aligned}$$

Example for the Ginzburg Landau equation

Example for the shear-driven cavity

# **System identification**



Natural dynamics

Actuators

$$\mathbf{x}_{i+1} = \mathbf{A} \mathbf{x}_i + \mathbf{B} \mathbf{u}_i$$

$$\mathbf{y}_i = \mathbf{C} \mathbf{x}_i + \mathbf{D} \mathbf{u}_i$$

Measurements

Feedthrough



$$\mathcal{O}_k = \begin{bmatrix} C \\ CA \\ CA^2 \\ CA^3 \\ \vdots \\ CA^{k-1} \end{bmatrix}$$

Observability

$$\mathcal{C}_k = [B \quad AB \quad A^2B \quad A^3B \quad \dots \quad A^{k-1}B]$$

Controlability

$$\mathcal{H}_k = [D \quad CB \quad CAB \quad CA^2B \quad CA^3B \quad \dots \quad CA^{k-1}B]$$

Markov parameters of the system

Schematic  
spring damper

mass

Impulse response

# EigenRealization Algorithm

$$\mathbf{y} = [y_1 \ y_2 \ y_3 \ y_4 \ y_5 \ y_6 \ y_7 \ y_8 \ y_9 \ y_{10}]$$

# EigenRealization Algorithm

$$\mathbf{H}_1 = \begin{bmatrix} y_1 & y_2 & y_3 & y_4 & y_5 \\ y_2 & y_3 & y_4 & y_5 & y_6 \\ y_3 & y_4 & y_5 & y_6 & y_7 \\ y_4 & y_5 & y_6 & y_7 & y_8 \\ y_5 & y_6 & y_7 & y_8 & y_9 \end{bmatrix}$$

# EigenRealization Algorithm

$$H_1 = \begin{bmatrix} CB & CAB & CA^2B & CA^3B & CA^4B \\ CAB & CA^2B & CA^3B & CA^4B & CA^5B \\ CA^2B & CA^3B & CA^4B & CA^5B & CA^6B \\ CA^3B & CA^4B & CA^5B & CA^6B & CA^7B \\ CA^4B & CA^5B & CA^6B & CA^7B & CA^8B \end{bmatrix}$$

# EigenRealization Algorithm

$$H_1 = \begin{bmatrix} C \\ CA \\ CA^2 \\ CA^3 \\ CA^4 \end{bmatrix} \begin{bmatrix} B & AB & A^2B & A^3B & A^4B \end{bmatrix}$$

# EigenRealization Algorithm

Observability:  $\mathcal{O} = U\Sigma^{\frac{1}{2}}$

Controlability:  $\mathcal{C} = \Sigma^{\frac{1}{2}}V^T$



# EigenRealization Algorithm

$$\mathbf{H}_2 = \begin{bmatrix} y_2 & y_3 & y_4 & y_5 & y_6 \\ y_3 & y_4 & y_5 & y_6 & y_7 \\ y_4 & y_5 & y_6 & y_7 & y_8 \\ y_5 & y_6 & y_7 & y_8 & y_9 \\ y_6 & y_7 & y_8 & y_9 & y_{10} \end{bmatrix}$$

# EigenRealization Algorithm

$$H_2 = \begin{bmatrix} C \\ CA \\ CA^2 \\ CA^3 \\ CA^4 \end{bmatrix} A \begin{bmatrix} B & AB & A^2B & A^3B & A^4B \end{bmatrix}$$

# EigenRealization Algorithm

## Natural dynamics

$$A = \mathcal{O}^\dagger H_2 \mathcal{C}^\dagger$$

## Actuators

$$B = \left[ \Sigma^{\frac{1}{2}} V^T \right]_{:,1:p}$$

## Measurements

$$C = \left[ U \Sigma^{\frac{1}{2}} \right]_{1:q,:}$$

## Feedthrough

$$D = y_0$$

## Mass spring damper example

## Cylinder flow example



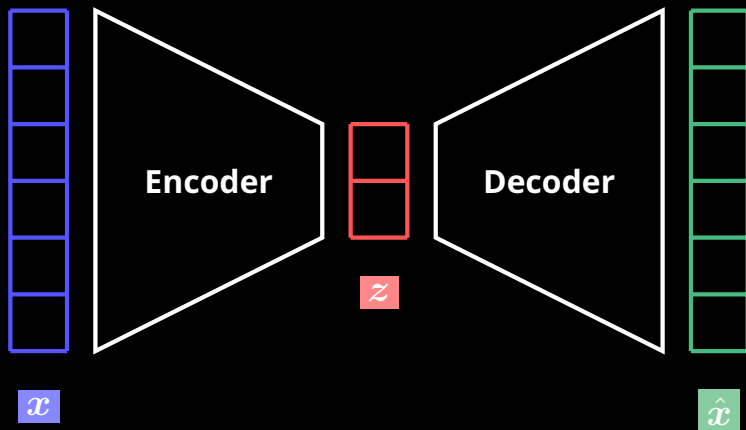
# **Conclusion**

Since the work of G. Golub *et al.* in the late 1960s, SVD plays a pivotal role in numerical linear algebra.

It is widely used in control theory to characterize various properties of input-output linear dynamical systems or for system identification purposes.



It also lays the foundation for the mathematical description of *quantum entanglement* in particle physics.



Many (linear) dimensionality reduction techniques in machine learning can actually be re-interpreted as variations around the theme of SVD.